RSC Advances

ROYAL SOCIETY OF CHEMISTRY

www.rsc.org/advances

Journal Name

ARTICLE

Thermal stable polyimide nanocomposite films from electrospinning $BaTiO_3$ fibers for high-density energy storage capacitors

Received 00th January 20xx,
Accepted 00th January 20xx

DOI: 10.1039/x0xx00000x

www.rsc.org/

Yun-Hui Wu,[a] Jun-Wei Zha,[a,b,c*] Zhi-Qiang Yao,[a] Fang Sun,[a] Robert K. Y. Li[b] and Zhi-Min Dang[a,*]

Barium titanate ($BaTiO_3$, BT) fibers were prepared via electrospinning with sol-gel precursor, followed by calcination process. Polyimide (PI) nanocomposite films with the electrospun BT fibers were fabricated using in situ dispersion polymerization method. The morphology and crystal structure of BT fibers were analyzed through scanning electron microscopy and X-ray diffraction. It was found that their diameter and length were greatly dependent on the calcination temperature. Compared to the spherical BT nanoparticles, the introduction of one-dimensional BT fibers into PI matrix gave rise to improved thermal stability. Besides, dielectric behaviors of the PI/BT-fiber composite films were investigated over the frequency range from 10^2 Hz to 10^6 Hz and within the temperature of 20 °C – 150 °C. The results demonstrated that the dielectric permittivity at 10^2 Hz of PI nanocomposite films with 30 vol% BT fibers was improved up to ~ 27, and the corresponding dielectric loss is relatively low (~ 0.015). The dielectric permittivity of the PI/BT-fiber composite films exhibited slight dependence on temperature, while highly dependent on the calcination temperature of electrospun BT fibers. This work opens a road to optimize the dielectric properties of thermosetting polymer composite films with high energy storage density.

1. Introduction

Polymer-based dielectric materials with high dielectric permittivity (ε) and low dielectric loss have attracted great attention in the fields of energy storage and electronic industry.[1] The addition of conductive particles into polymer matrices has been reported for improving the dielectric permittivity.[2,3] Dielectric permittivity of the composites can be significantly improved when the filler fraction is close to percolation threshold. But their dielectric loss also seems to be sharply increased due to the formation of conductive networks, which limits their usage in electronic devices. In general, polymers filled with high ε ceramic fillers have been considered as promising materials to fabricate high ε polymer composites.[4,5]

Owing to their excellent dielectric and ferroelectric properties, nanostructured barium titanate ($BaTiO_3$, BT) fillers and BT based nanocrystals such as Barium strontium titanate (BST) have been employed in polymer-matrix composites, giving rise to improve dielectric permittivity and to lower dielectric loss.[6-8] Fan et al. reported that PI nanocomposite films filled BT nanoparticles with three kinds of diameters were prepared and argued that the roles of nanoparticles such as size and crystal phase has great influence on the dielectric behaviors.[9] Li et al investigated the dielectric properties of polyvinylidene-fluoride (PVDF) nanocomposites with embedded BST/silver core/shell nanoparticles. The relative permittivity of composites was significantly increased to 153 at 100 Hz while the loss tangent was kept low.[10] It is well know that the filler morphology (size, shape, aspect ratio, etc) plays an important role on the properties of polymer composite. In recent years, one-dimensional (1D) materials such as fibers, nanowires, nanotubes and nanorods have been focused on to prepare composites with a wide range of applications due to their small size, high surface-to-volume ratio, high density of surface sites, and unique chemical and physical properties.[11-14] Compared to spherical BT particles, the BT fibers with larger aspect ratios and dipolar movement along the longitudinal axis could give rise to improving dielectric properties of the composites at the same concentration of BT loading.

Electrospinning is a simple and effective method for preparing one-dimensional material systems, including metal oxides, ceramics, polymers, and composites.[15-17] It is worth noting that BT fibers have been successfully synthesized via electrospinning.[18,19] It is known that the properties of ceramic fillers (particles) are related to their crystallization and microstructure. In the fabrication of electrospun ceramic fibers, organic binder removal and calcination need to be carried out under elevated temperature. However, the

[a] Laboratory of Dielectric Polymer Materials and Devices, Department of Polymer Science and Engineering, University of Science and Technology Beijing, Beijing 100083, People's Republic of China.
E-mail: zhajw@ustb.edu.cn, dangzm@ustb.edu.cn Tel: +86-10-62334516
[b] Department of Physics and Materials Science, City University of Hong Kong, Kowloon, Hong Kong, People's Republic of China
[c] State Key Laboratory of Power Transmission Equipment & System Security and New Technology, Chongqing University, Chongqing, 400030, P. R. China

influences of the calcination condition on the morphology and crystal structure of the BT fibers and their composites might affect the dielectric properties, which have not been properly investigated until now.

In this work, the BT fibers were prepared by electrospinning and calcination. Due to its outstanding dielectric and mechanical properties, as well as high thermal and chemical stability, polyimide (PI) was selected as polymer matrix. The PI nanocomposite films with electrospun BT fibers were prepared using in situ dispersion polymerization process. The microstructures and crystal phases of BT fibers at different calcination temperatures were investigated. And their influence on dielectric properties of the nanocomposite films was discussed. Finally, the high ε and low dielectric loss thermosetting polymer films with high thermal stability and potentially high energy storage density are realized in this work.

2. Experimental

2.1 Material

Barium acetate (99%, Xilong chemical Co. Ltd.), tetrabutyl titanate (98.5%, Beijing Xingjin Chemical Corp.), glacial acetic acid (99.5%, Sinopharm Chemical Reagent Co., Ltd.), poly(vinyl pyrrolidone) (PVP, 95%, Beijing BioDee Bio Tech Co. Ltd.) were used to prepare the BT fibers. Pyromellitic dianhydride (PMDA, 98.5%) and 4, 4′ -oxydianiline (ODA, 98%) were purchased from Sinopharm Chemical Reagent Co. Ltd, China. N, N′ -dimethylacetamide (DMAc, 99.5%) provided by Beijing Chemical Corp., China was used as solvent to prepare the composites. The mole ratio of PMDA and ODA is set as 1.02:1.

2.2 Preparation of the BT fibers

The as-received barium acetate was dissolved in glacial acetic acid, and tetrabutyl titanate was dropwise added into the mixture. The mole ratio of barium acetate to tetrabutyl titanate was set as 1:1.2. The obtained suspension sol was mixed with PVP in ethanol, and magnetically stirred for 2 h. Then the evenly dispersed precursor was filled into a plastic syringe. During the electrospinning process, a direct current (DC) voltage of 18 kV was applied to the needle by a power supply unit and the syringe pump fed the sol at a constant rate of 0.06 mm/min. The distance between the needle tip and collecting plate was set as 10 cm. The electrospun fibers were collected on an aluminum foil attached to the collector. Schematic of the electrospinning process used in this study were illustrated in Fig. 1. Subsequently, they were calcined at 600 °C, 800 °C and 1000 °C for 1 h in air, respectively.

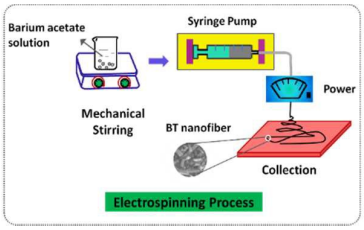

Fig. 1 Schematic illustration of the electrospinning setup used.

2.3 Preparation of the PI/BT nanocomposite films

The PI/BT nanocomposite films were fabricated using in situ dispersing polymerization. First, the BT fibers and ODA were stirred for 10 min in DMAc solvent and then PMDA was added into the suspension. The mixture was stirred for 4 h at this viscosity to obtain poly(amic acid) (PAA) suspension with uniformly dispersed BT fibers. Finally, the suspension was cast onto a clean glass plate and degassed under vacuum at room temperature to eliminate the entrapped air and the remaining ethanol. The PAA could be converted to PI by thermal imidization as follows: 60 °C for 1 h, 100 °C for 1 h, 200 °C for 1 h, 300 °C for 1 h, respectively. Finally, the PI/BT-fiber compoiste films were obtained. All as-prepared composite films were controlled in the thickness of ~ 50 μm. For comparison, the PI composite films filled with BT nanoparticles were also prepared using the same process.

2.4 Characteristics

Crystal phase structures of the BT fibers were characterized by an X-ray diffraction instrument (Japan RigakuD/max-RC) over the 2θ of 10° to 80°. Morphology of the BT fibers and PI nanocomposite films were characterized by scanning electron microscopy (SEM, HITACHI S-4700). Fourier transform infrared (FT-IR) spectra were measured using a Nicolet IS10 spectrometer by incorporating the samples in a KBr disk. Thermalgravimetric analysis (TGA) of the samples was carried out by using TA Instruments Taq 50 from 20 °C to 800 °C with a heating rate of 10 °C/min under nitrogen atmosphere. Dielectric properties of the PI nanocomposite films were measured using an impedance analyzer (Agilent 4294A) in the frequency range from 10^2 Hz to 10^6 Hz and the temperature of 20 °C – 150 °C. Prior to measurement, the silver paste was applied on both sides of the PI nanocomposite films to ensure good electrical contact.

3. Results and discussion

The influences of calcination temperatures on the morphology of BT fibers are investigated by SEM. Fig. 2a~c show the SEM images of as-electrospun BT fibers calcined at 600 °C, 800 °C and 1000 °C. It can be seen that the diameter and length of BT fibers are greatly dependent on the calcination temperature. As the temperature increases from 600 to 1000 °C, the average diameter of $BaTiO_3$ fibers gradually decreases from ~ 600 nm to ~ 300 nm. However, the length of BT fibers increases with the increase of calcination temperature. We can see that their length is about 3 μm, 4 μm, and 6 μm when calcined at 600 °C, 800 °C and 1000 °C, respectively. Fig. 3d presents TEM images of BT fibers calcined at 1000 °C. It can be observed that the BT fiber is smooth and highly aligned. Moreover, there is no aggregations can be seen.

To observe the phase transformation with temperature, XRD patterns of the BT fibers calcined at 600 °C, 800 °C and 1000 °C are shown in Fig. 3a. It can be seen that most peaks of

the as-synthesized BT fibers can well match the standard pattern of BT spectra (PDF#75-0462), and there is no impurity phase in all the three patterns. Meanwhile, it can also be found that the diffraction peaks of BT fibers become sharper with increasing the calcination temperature, suggesting that high calcination temperature will give rise to better crystallization. With regard to the XRD patterns of samples calcined at 600 °C and 800 °C, all the diffraction peaks are considered to be the cubic phases. For the BT fibers calcined at 1000 °C, it is worth noting that the characteristic splitting of the peaks at 2θ=44–46° as shown in Fig. 3a corresponding to the (002) and (200) planes of tetragonal phase. Besides, as shown in the magnification of 2θ=44–46° zone (in Fig. 3b), there is obvious difference of the peak breadth of the samples treated at 1000°C compared to those at 600°C to 800 °C. It suggests that the increase of calcination temperature can make the phase of BT fibers gradually transform from cubic to tetragonal phase. On the other hand, with the calcination temperature increased from 600°C to 800 °C, it can be observed that the peak intensities become higher, implying the better crystallization during the calcination process.

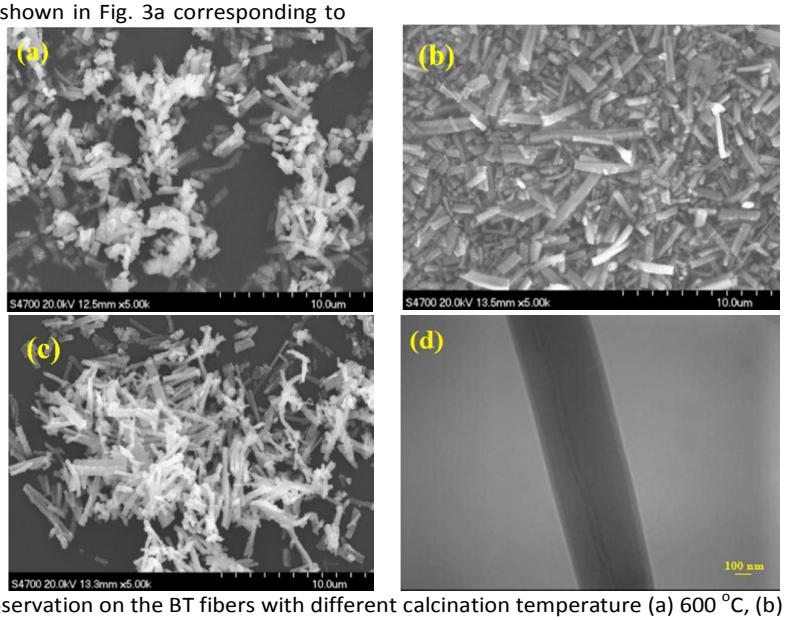

Fig. 2 SEM observation on the BT fibers with different calcination temperature (a) 600 °C, (b) 800 °C and (c) 1000°C, and (d) TEM image of the BT fibers with the calcination temperature of 1000 °C.

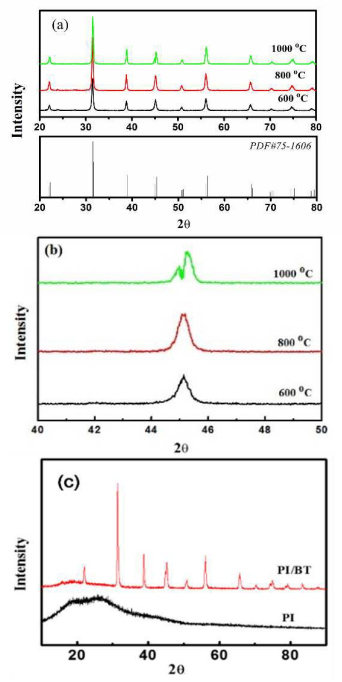

Fig. 3 XRD patterns of (a) the BT fibers with different calcination temperature at 600 °C, 800 °C and 1000 °C, respectively, (b) 2θ from 40° to 50°, (c) the pure PI films and PI composite films with 10 vol% BT fibers loading.

XRD patterns of pure PI films and PI nanocomposite films with 10 vol% BT fibers loading are shown in Fig. 3c. For pure PI films, it can be seen that there is a broad peak which starts from about 2θ=17.8°. This broad peak can be attributed to the regular arrangement of PI polymer chain. However, a broad peak starting from about 2θ=15.8° can be observed in the PI/BT-fiber composite films, indicating the increase of averaged interplanar distance of polymer resulted from the incorporation of BT fibers. The chemical structure of BT fibers, pure PI film and the PI/BT-fiber composite films are characterized using FTIR as shown in Fig. 4a. The characteristic peaks of symmetric C=O stretching, asymmetric C=O stretching, and C=N stretching of the imide group are clearly visible at about 1720 cm^{-1}, 1780 cm^{-1}, and 1380 cm^{-1}, respectively. The absorption peak near 1650 cm^{-1} disappears in the spectra of all the films (carbonyl group in PAA). These results indicate that the imidization of nanocomposite films could not be impeded by the presence of the BT fibers.

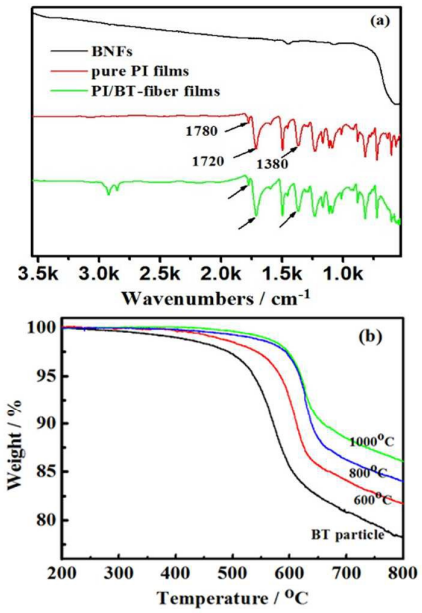

Fig. 4 (a) FTIR spectra of the (1) BT fibers, (2) pure PI films, and (3) PI/BT-fiber composite films, and (b) TGA curves of PI/BT composite films with BT fibers and nanoparticles.

Table 1 Characteristic temperatures of the PI composite films obtained from TGA curves at heating rate of 10 °C/min under N_2.

Fillers	T_5	T_m
BT particles	535	576
BT fibers (600°C)	582	606
BT fibers (800°C)	616	625
BT fibers (1000°C)	618	628

T_5: degradation temperature at 5% mass loss; T_m: temperature at maximum rate of mass loss.

Fig. 4b shows thermogravimetric analysis (TGA) curves of the PI nanocomposite films with BT fibers and nanoparticles loading. Table 1 lists the characteristic temperatures of the PI nanocomposite films determined from TGA curves. It is clearly observed that the thermal decomposition temperature of PI/BT-fiber composite films is higher than that of PI/BT-nanoparticle ones. For the PI/BT-fiber composite films, their decomposition shifts to higher temperature with increasing calcination temperature (see T_5 listed in Table 1). And the composites filled with BT fibers (1000 °C) show the higher temperature (628 °C) at maximum rate of mass loss (T_m). The residual weight of the composites at 750 °C also increased with increasing the calcination temperature. Therefore, it could be concluded that the BT fibers calcined at high temperature leads to higher thermal stability of the PI/BT-fiber composite films. The BT fibers calcined at higher temperature have larger specific surface area, possibly giving rise to the improved interfacial fiber/matrix interaction. This will restrict the thermal motion of PI chains, thus resulting in more stable thermal properties of the PI/BT-fiber composites.

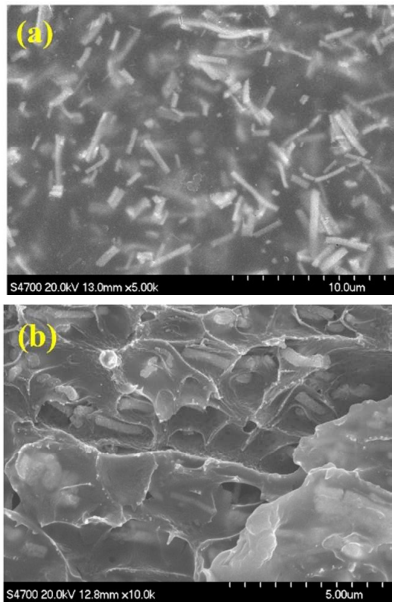

Fig. 5 SEM images of (a) surface and (b) fracture section of the PI composite films with 10 vol% BT fibers loading.

Fig. 5 shows the surface and fracture section morphologies of PI/BT-fiber composite films with 10 vol% BT fibers calcined at 1000 °C. It reveals that the BT fibers are evenly dispersed in the PI matrix and the BT fiber networks can be well formed between the neighboring fibers. Besides, good interfacial interaction between BT fibers and PI matrix can be observed. The existence of this interfacial interaction possibly gives rise to more interfacial polarization of the composite system, which can lead to the Maxwell-Wagner-Sillars (MWS) effect.[16] It is well known that the dielectric properties of materials are closely related to the molecular polarization. Thus, the interfacial polarization between BT fibers and PI matrix would play an important role in improving the dielectric properties of the PI/BT-fiber composite films.

Dielectric properties of the ceramic filled polymer composites are influenced not only by the inherent dielectric properties of polymer and ceramic phases, but also the ceramic morphologies in the polymer matrix. Generally, the 1D fibers are considered to be able to increase the dielectric permittivity more efficiently than the spherical fillers. It is found that dielectric permittivity and dielectric loss increase with BT fibers concentration as shown in Fig. 6a and 6b. The ε of PI/BT-fiber composite films is up to 26.6 when the content of BT fibers is 30 vol% as shown in Fig. 6a. In comparison with pure PI film (ε = 3.2), the dielectric permittivity of the composite is nearly 8 times higher than that of pure PI. This value is much larger than that of PI/BT hybrid films (ε = 18.35) with 40 vol% BT nanopartilces.[17] It can also be observed that the ε of PI/BT-fiber composite films is higher than that of PI/BT-nanoparticle composite films with the concentration of 30 vol%, and the calcination temperature takes a great effect on the ε of PI/BT-fiber composite films, as shown in Fig. 6c. The ε of PI composite films with BT fibers calcined at 1000 °C is higher than that of films with BT fibers calcined at 600 °C and

800 °C, which is attributed to the tetragonal phase formed at 1000 °C calcination temperature (Fig. 3a and 3b). In addition, the increase of interface and contact between filler and matrix would lead to an improvement of electron mobility and interface polarization, which results in larger dielectric permittivity of the composites.

The dielectric loss PI/BT-fiber composite film is 0.015 when the 10 vol% BT fibers is loaded and it reaches the highest value of 0.10 at 30 vol% BT fibers loading. The increase of dielectric loss is attributed to clusters of BT fibers in the polymer matrix. It shows that when BT fibers is 10 vol%, dielectric loss of the composite film does not show a large increase, indicating that there is no accumulation of interfacial charges inside the composites. A clear frequency dependence is observed for the PI nanocomposite film with 30 vol% BT fibers loading, which is mainly attributed to the remarkably interfacial polarization or commonly referred to MWS polarization between BT fibers and PI matrix.

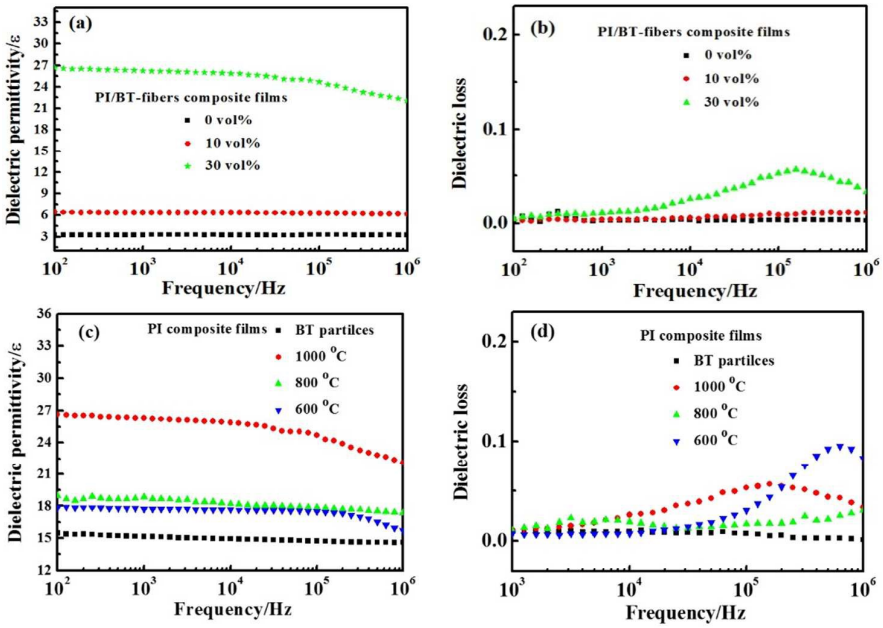

Fig. 6 Frequency dependence of dielectric property of the PI composite films on (a), (b) the volume fraction of the BT fibers and (c), (d) 30 vol% BT fibers and nanoparticles measured at room temperature.

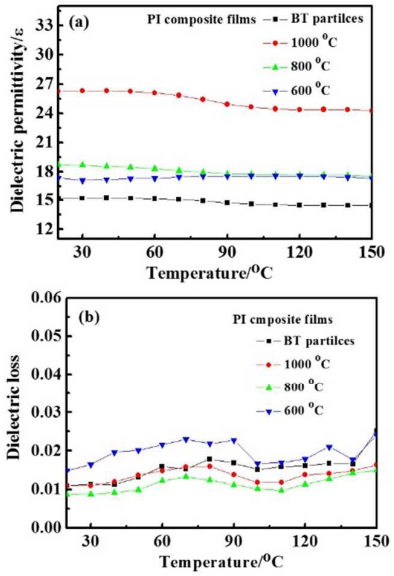

Fig. 7 Temperature dependence of dielectric permittivity (a) and dielectric loss (b) of the PI composite films with 30 vol% BT fibers and nanoparticles measured at f=10^2 Hz.

In order to identify the influence of temperature on dielectric behavior of the PI/BT-fiber composite films, the dielectric permittivity and dielectric loss were measured in the temperature range from 20 °C to 150 °C as shown in Fig. 7. The ε and dielectric loss of PI/BT-fiber composite films exhibit a weak temperature dependence as shown in Fig. 7a and 7b. It can be concluded that PI matrix has excellent thermal properties whose glass transition temperature (Tg) is about 350 oC.18,19 Both the mobility and thermal expansion of the polymer have an effect on the dielectric properties. However, the BT fibers loaded in the PI matrix form more contact networks which could restrict the chain mobility and thermal expansion of the PI matrix. Thus the ε and dielectric loss do not remarkable change over the temperature range.

Energy density of the pure PI film and PI nanocomposite films with different BT fillers loading is shown in Fig. 8a. It is notable that the energy density of PI nanocomposite films is higher than that of pure PI film and the energy density of PI nanocomposite films with BT fibers calcined at 1000 °C is the highest one.

As we know, the maximum energy density, *W*, can be described as follows.[24,25]

$$W = \frac{1}{2}\varepsilon_0 \varepsilon E_b^2 \quad (1)$$

where ε_0 is the vacuum dielectric permittivity of 8.85×10^{-12} F m^{-1}, ε is the dielectric permittivity of the samples, E_b is the breakdown strength. According to Eq. (1), besides a high E_b, a high ε is another key factor in realizing a high energy density. It should also be noted that for the films studied here, E_b is replaced by E_{test} which is the test electric field of dielectric property measurement. Thus, the energy density can be written as follows.

$$W = \frac{1}{2}\varepsilon_0 \varepsilon E_{test}^2 \quad (2)$$

Because the testing voltage is constant and all the samples have the same thickness of ~ 50 μm, E_{test} is the constant in this study. Therefore, the higher energy density is attributed to the higher ε (at 100 Hz) of the samples. The results demonstrate the advantage of the PI/BT-fiber composite films that exhibit excellent dielectric property significantly showing high energy density. Temperature dependency of the energy density is also shown in Fig. 8b. It can be noted that the energy density does not remarkable change over the temperature range due to the thermal stability of PI matrix. Hence, these electrospun fibers filled PI nanocomposites can provide a new approach for developing high-density energy storage capacitors.

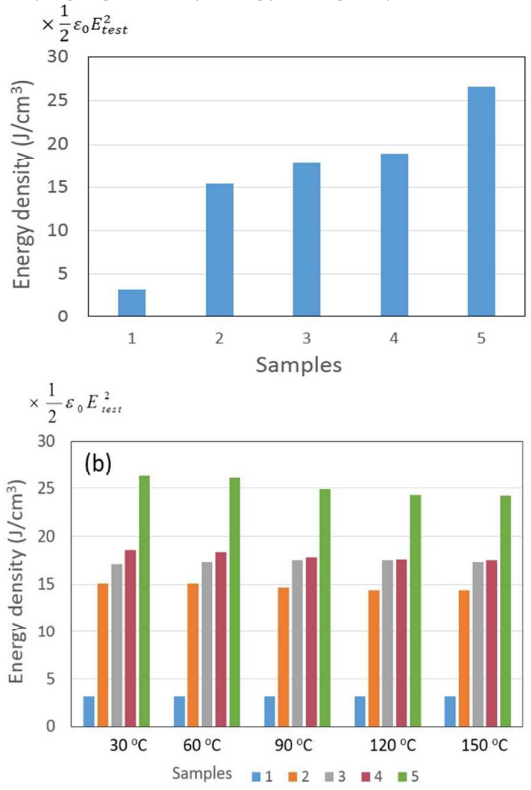

Fig. 8 Energy density of (a) pure PI film and PI composite films with 30 vol% BT fillers loading and (b) Energy density of the samples vs. temperature. Samples 1, 2, 3, 4, and 5 represent the pure PI film, PI/BT-particles, PI/BT-fiber (600 °C), PI/BT-fiber (800 °C) and PI/BT-fiber (1000 °C), respectively.

4. Conclusions

In summary, PI composite films with electrospun BT fibers were fabricated using the in situ dispersion polymerization method. The microstructures, thermal and dielectric properties of the BT fibers and composite films were investigated. The diameters and lengths of BT fibers are closely related to their calcined temperature. Compared to the traditional PI/BT-nanoparticle composite films, the introduction of BT fibers into PI matrix gave rise to better thermal stability and higher dielectric permittivity. Moreover, the dielectric permittivity of the composite films exhibited large dependence on the BT calcination temperature and weak temperature dependence. The neighboring BT fibers could easily form contact networks in the matrix, which induced the noticeable interfacial polarization. Thus, the addition of BT fibers resulted in the improved dielectric properties, which was demonstrated to be effective way to enhance the high energy density for PI/BT-fiber composite films. These results show the potential to tailor the dielectric properties of the materials for the applications in high energy density capacitors.

Acknowledgements

The financial support from the NSFC (No. 51207009 and 51377010), Ministry of Education of China through Doctor Project (Grant No. 20130006130002), National Basic Research Program of China (973 Program, 2014CB239503), the Hong Kong Scholar Program (XJ 2014048), Fundamental Research Funds for the Central Universities (No. FRF-TP-14-016A2), and Visiting Scholarship of State Key Laboratory of Power Transmission Equipment & System Security and New Technology (Chongqing University) (2007DA10512714407).

References

1 Z. M. Dang, J. K. Yuan, J. W. Zha, T. Zhou, S. T. Li, G. H. Hu, *Progr. Mater. Sci.*, 2012, **57**, 660.
2 L. Zhang, W. Wang, X. Wang, P. Bass, Z. Y. Cheng, *Appl. Phys. Lett.*, 2013, **103**, 232903.
3 A. B. da Silva, M. Arjmand, U. Sundararaj, R. E. S. Bretas, *Polymer*, 2014, **55**, 226.
4 Z. M. Dang, T. Zhou, S. H. Yao, J. K. Yuan, J. W. Zha, H. T. Song, J. Y. Li, Q. Chen, W. T. Yang, J. Bai, *Adv. Mater.*, 2009, **21**, 2077.
5 F. He, S. Lau, H. L. Chan, J. Fan, *Adv. Mater.*, 2009, **21**, 710.
6 B. H. Fan, J. W. Zha, D. Wang, J. Zhao, Z. M. Dang, *Appl. Phys. Lett.*, 2012, **100**, 012903.
7 M. E. Hossain, S. Liu, J. Li, S. O'Brien, *Nanotechnology*, 2013, **1**, 554.
8 K. Osin´ska, D. Czekaj, J Therm Anal Calorim, 2013, **113**, 69.
9 B. H. Fan, J. W. Zha, D. R. Wang, J. Zhao, Z. F. Zhang and Z. M. Dang, Comp. Sci. Technol., 2013, **80**, 66.
10 K. Li, H. Wang, F. Xiang, W. Liu, and Haibo Yang, Appl. Phys. Lett., 2009, 95, 202904.
11 Y. Song, Y. Shen, P. Hu, Y. Lin, M. Li, and C. W. Nan, Appl. Phys. Lett., 2012, 101, 152904.
12 Z. Spitalsky, D. Tasis, K. Papagelisb, C. Galiotis, *Progr. Polym. Sci.*, 2010, **35**, 357.

13 A. Allaoui, S.V. Hoa, M. D. Pugh, *Compos. Sci. Technol.*, 2008, 68, 410.
14 H. Tang, Y. Lin, C. Andrews, H. A Sodano, *Nanotechnology*, 2011, **22**, 015702.
15 L. Q. Liu, D. Tasis, M. Prato, H. D. Wagner. *Adv. Mater.*, 2007, **19**, 1228.
16 S. Agarwal, A. Greiner, J. H. Wendorff, *Progr. Polym. Sci.*, 2013, **38**, 963.
17 S. H. Choi, G. Ankonina, D. Y. Youn, S. G. Oh, J. M. Hong, A. Rothschild, II D. Kim, *ACS Nano*, 2009, **3**, 2623.
18 J. Yuh, J. C. Nino, W. M. Sigmund, *Mater. Lett.*, 2005, **59**, 3645.
19 H. Li, H. Wu, D. Lin, W.Pan. *J. Am. Ceram. Soc.*, 2009, **92**, 2162.
20 P. Hedvig, Dielectric Spectroscopy of Polymer, Adam Hilger, Bristol, 1977.
21 Z. M. Dang, Y. Q. Lin, H. P. Xu, C. Y. Shi, S. T. Li, J. Bai, *Adv. Funct. Mater.*, 2008, **18**, 1509.
22 S. H. Hsiao, Y. J. Chen, *Europ. Polym. J.*, 2002, **38**, 815.
23 J. W. Zha, Z. M. Dang, T. Zhou, H. T. Song, G. Chen, *Synth. Metals*, 2010, **160**, 2670.
24 B. Chu, X. Zhou, K. Ren, B. Neese, M. Lin, Q. Wang, F. Bauer, Q. M. Zhang, *Science*, 2006, **313**, 334.
25 X. Hao, *J. Adv. Dielect.*, 2013, **3**, 1330001-1.